nature medicine

Sirt1 mediates neuroprotection from mutant huntingtin by activation of the TORC1 and CREB transcriptional pathway

Hyunkyung Jeong[1,5], Dena E Cohen[2,5], Libin Cui[1], Andrea Supinski[2], Jeffrey N Savas[3], Joseph R Mazzulli[1], John R Yates III[3], Laura Bordone[4], Leonard Guarente[2] & Dimitri Krainc[1]

Sirt1, a NAD-dependent protein deacetylase, has emerged as a key regulator of mammalian transcription in response to cellular metabolic status and stress[1]. Here we show that Sirt1 has a neuroprotective role in models of Huntington's disease, an inherited neurodegenerative disorder caused by a glutamine repeat expansion in huntingtin protein (HTT)[2]. Brain-specific knockout of Sirt1 results in exacerbation of brain pathology in a mouse model of Huntington's disease, whereas overexpression of Sirt1 improves survival, neuropathology and the expression of brain-derived neurotrophic factor (BDNF) in Huntington's disease mice. We show that Sirt1 deacetylase activity directly targets neurons to mediate neuroprotection from mutant HTT. The neuroprotective effect of Sirt1 requires the presence of CREB-regulated transcription coactivator 1 (TORC1), a brain-specific modulator of CREB activity[3]. We show that under normal conditions, Sirt1 deacetylates and activates TORC1 by promoting its dephosphorylation and its interaction with CREB. We identified BDNF as a key target of Sirt1 and TORC1 transcriptional activity in both normal and Huntington's disease neurons. Mutant HTT interferes with the TORC1-CREB interaction to repress BDNF transcription, and Sirt1 rescues this defect *in vitro* and *in vivo*. These studies suggest a key role for Sirt1 in transcriptional networks in both the normal and Huntington's disease brain and offer an opportunity for therapeutic development.

Recent evidence suggests that Sirt1, a member of sirtuin family that has been implicated in aging and metabolism, has a neuroprotective role in neurodegenerative disorders[1]. However, the exact nature of normal Sirt1 function in the mammalian brain has not been ascertained. To clarify the function of Sirt1 in the brain and to determine its contribution to neurodegeneration, we focused on Huntington's disease, an autosomal dominant disease that commonly presents in adult life and includes personality changes, cognitive changes, psychiatric disturbances and abnormal movements[2]. Huntington's disease belongs to a family of polyglutamine disorders that, in addition to the expanded polyglutamine repeats, share a number of features, such as adult onset, progressive neurodegeneration, an inverse correlation of the number of polyglutamine repeats with age of onset and the presence of polyglutamine protein-containing inclusions[2]. Polyglutamine diseases, including Huntington's disease, are fatal, as there are no effective treatments to cure these diseases or slow their progression.

The role of Sirt1 in Huntington's disease has been previously studied in *Drosophila melanogaster* and *Caenorhabditis elegans*, but the results from these studies have been contradictory. For example, in *C. elegans* worms overexpressing Sir2 (the ortholog of human Sirt1), *HTT*-induced neurodegeneration is suppressed, whereas overexpression of Sir2 in the *D. melanogaster* fly model of Huntington's disease confers no substantial neuroprotection[4,5]. To examine the role of Sirt1 in Huntington's disease mice, we first crossed a conditional allele of Sirt1 ($Sirt1^{flox}$) with the Nestin-Cre driver to yield knockout of Sirt1 in the brain (brain-specific knockout (BSKO), $Sirt1^{flox/flox}$; Nestin-Cre). These mice were born at Mendelian ratios and had no gross defects in brain development[6]. To determine the impact of the ablation of neuronal Sirt1 on Huntington's disease, we then crossed BSKO mice with the R6/2 mouse model of Huntington's disease[7]. These crosses, which we carried out on an inbred C57BL/6 background, yielded $Sirt1^{flox/flox}$ controls (referred to as WT) and $Sirt1^{flox/flox}$; R6/2 (R6/2), $Sirt1^{flox/flox}$; Nestin-Cre (BSKO) and $Sirt1^{flox/flox}$; Nestin-Cre–R6/2 (BSKO-R6/2) mice. Behavioral experiments revealed a significant acceleration of motor deficits in BSKO-R6/2 mice compared to R6/2 mice, as assessed by rotarod performance (**Fig. 1a** and **Supplementary Fig. 1a**). To determine whether neuropathological alterations accompanied this behavioral phenotype, we performed an unbiased stereological analysis of brain sections. Previous studies have shown that R6/2 mice show a progressive atrophy of striatal neurons that resembles the neuropathology observed in human Huntington's disease[8]. R6/2 mice showed significant striatal atrophy compared to WT mice (**Fig. 1b**). BSKO mice, which are smaller than WT mice[6], also had smaller striata than the WT mice. BSKO-R6/2 mice had significantly smaller striatal volume compared to BSKO or R6/2 mice (**Fig. 1b**). In addition, when analyzing a series of sections spanning the striatum, we observed a significantly lower mean neuronal volume in the striata of the BSKO-R6/2 mice compared to R6/2 mice (**Fig. 1c**). To examine the aggregation of mutant HTT, we looked at the mean aggregate count in all

[1]Department of Neurology, Massachusetts General Hospital, MassGeneral Institute for Neurodegenerative Disease, Harvard Medical School, Charlestown, Massachusetts, USA. [2]Paul F. Glenn Laboratory, Department of Biology, Massachusetts Institute of Technology, Cambridge, Massachusetts, USA. [3]Department of Chemical Physiology, The Scripps Research Institute, La Jolla, California, USA. [4]Cardiovascular and Metabolism Disease Area, Novartis Institutes for BioMedical Research, Cambridge, Massachusetts, USA. [5]These authors contributed equally to this work. Correspondence should be addressed to D.K. (krainc@helix.mgh.harvard.edu) or L.G. (leng@mit.edu).

Received 12 January; accepted 14 October; published online 18 December 2011; doi:10.1038/nm.2559

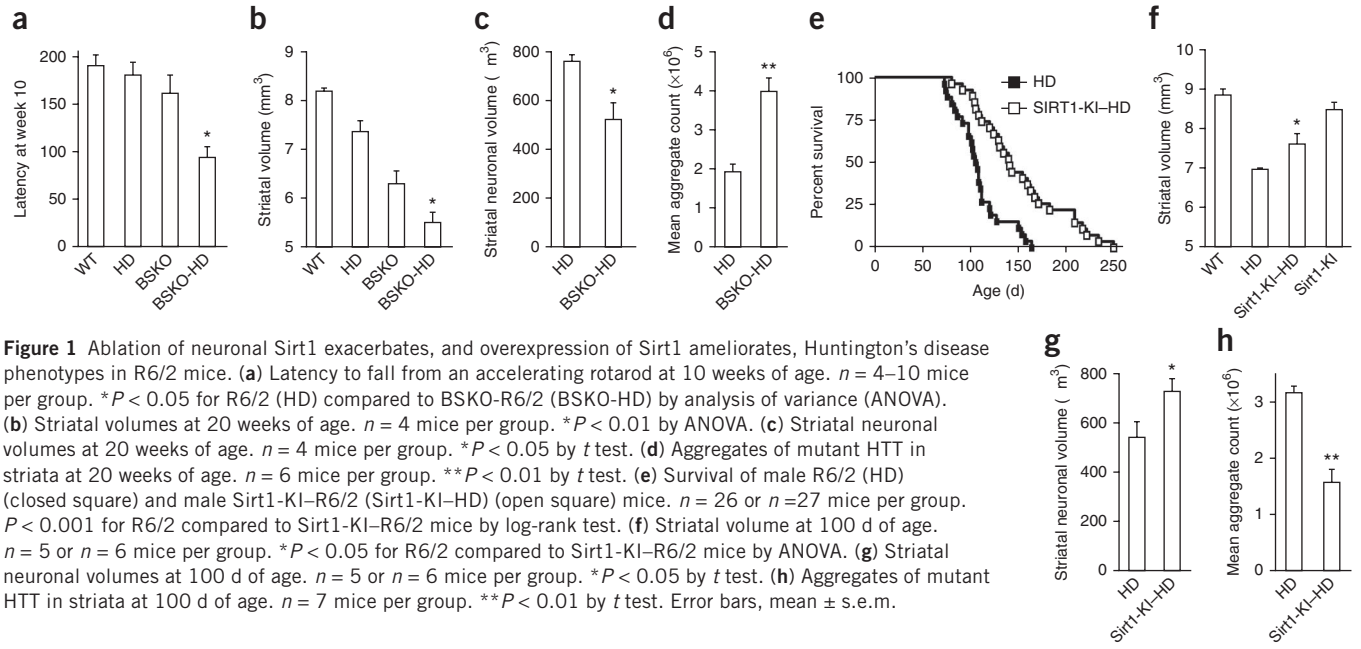

Figure 1 Ablation of neuronal Sirt1 exacerbates, and overexpression of Sirt1 ameliorates, Huntington's disease phenotypes in R6/2 mice. (**a**) Latency to fall from an accelerating rotarod at 10 weeks of age. $n = 4$–10 mice per group. $^*P < 0.05$ for R6/2 (HD) compared to BSKO-R6/2 (BSKO-HD) by analysis of variance (ANOVA). (**b**) Striatal volumes at 20 weeks of age. $n = 4$ mice per group. $^*P < 0.01$ by ANOVA. (**c**) Striatal neuronal volumes at 20 weeks of age. $n = 4$ mice per group. $^*P < 0.05$ by t test. (**d**) Aggregates of mutant HTT in striata at 20 weeks of age. $n = 6$ mice per group. $^{**}P < 0.01$ by t test. (**e**) Survival of male R6/2 (HD) (closed square) and male Sirt1-KI–R6/2 (Sirt1-KI–HD) (open square) mice. $n = 26$ or $n = 27$ mice per group. $P < 0.001$ for R6/2 compared to Sirt1-KI–R6/2 mice by log-rank test. (**f**) Striatal volume at 100 d of age. $n = 5$ or $n = 6$ mice per group. $^*P < 0.05$ for R6/2 compared to Sirt1-KI–R6/2 mice by ANOVA. (**g**) Striatal neuronal volumes at 100 d of age. $n = 5$ or $n = 6$ mice per group. $^*P < 0.05$ by t test. (**h**) Aggregates of mutant HTT in striata at 100 d of age. $n = 7$ mice per group. $^{**}P < 0.01$ by t test. Error bars, mean ± s.e.m.

four genotypes. Although no aggregates were present in WT or BSKO mice, the number of mutant HTT aggregates was significantly larger in BSKO-R6/2 compared to R6/2 mice (**Fig. 1d**). These results show that deficiency of Sirt1 accelerates neurodegeneration in Huntington's disease mice.

To test whether increased expression of Sirt1 might provide neuroprotection in the R6/2 model of Huntington's disease, we took advantage of a transgenic mouse that overexpresses Sirt1 under the control of the endogenous β-actin promoter (Sirt1-KI)[9]. These transgenic mice, which are maintained on an outbred genetic background, overexpress Sirt1 in a variety of tissues, including the brain, where Sirt1 is overexpressed approximately twofold in both the cortex and striatum; however, this overexpression was less pronounced in female than in male Sirt1-KI mice (**Supplementary Fig. 1b**,**c**). We crossed Sirt1-overexpressing mice (Sirt1-KI/+) with R6/2 mice to generate wild-type (WT), Sirt1-KI, unmodified R6/2 and Sirt1-overexpressing R6/2 (Sirt1-KI–R6/2) mice. These four groups were born at the expected Mendelian ratios. An analysis of body weight loss and rotarod performance revealed that Sirt1 overexpression was unable to provide protection against these outcome measures in the R6/2 mouse (**Supplementary Fig. 1d**,**e**). However, we found that Sirt1 overexpression significantly ($P < 0.001$) extended the survival time of R6/2 mice from an average of 100 d to an average of 130 d (**Fig. 1e**). Notably, we observed this effect only in male mice, whereas female mice showed no differences in survival time (**Supplementary Fig. 1f**). Although the precise reasons for this gender-specific effect are unclear, it is possible that lower Sirt1 overexpression in female Sirt1-KI mice had a role (**Supplementary Fig. 1c**). Notably, Sirt1 overexpression did not extend the lifespan of otherwise normal mice (**Supplementary Fig. 2**), indicating that the lifespan extension provided by this strain is specific to Huntington's disease. A neuropathological analysis revealed significant striatal and neuronal atrophy in R6/2 mice compared to either WT or SIRT1-KI mice (**Fig. 1f**,**g**). However, the degree of both the striatal and neuronal atrophy was significantly reduced in SIRT1-KI–R6/2 mice compared to R6/2 mice, indicating that overexpression of Sirt1 protected against striatal degeneration in this model (**Fig. 1f**,**g**). Further, an analysis of mutant HTT aggregate formation revealed that Sirt1-KI–R6/2 mice had a significantly reduced aggregate burden compared to R6/2 mice (**Fig. 1h** and **Supplementary Fig. 3**). These results indicate that Sirt1 overexpression can protect against key neuropathological phenotypes in the R6/2 Huntington's disease mouse model.

Having shown that overexpression of Sirt1 protects against mutant HTT toxicity *in vivo*, we asked whether this protection was a result of the direct effects of Sirt1 on neurons. Using lentiviral expression in primary cortical neurons, we achieved high transduction efficiency (>90%) and predominantly neuronal expression of the transduced constructs (**Supplementary Fig. 4a**). We used neurofilament staining to detect degeneration of neurites as an early marker of neuronal toxicity[10]. These experiments revealed a progressive loss of neurofilament staining that correlated with the duration of exposure of the primary neurons to mutant HTT (**Supplementary Fig. 4b**). Lentiviral expression of mutant HTT with 72 glutamines resulted in a significant loss of neurites compared to expression of WT HTT that had a nonexpanded polyglutamine tract (**Fig. 2a**,**b**). Expression of lentiviral Sirt1 significantly rescued the neuronal toxicity of mutant HTT despite the fact that only about 70% of the neurons expressed both Sirt and mutant HTT (**Fig. 2a**,**b**). This protection was mediated by the deacetylase activity of Sirt1, as the deacetylase-deficient Sirt1 mutant H363Y (Sirt1 HY) did not show significant neuroprotection compared to WT Sirt1 (**Fig. 2b**). Using nuclear staining of neurons as a readout, we found that Sirt1 also protected from the mutant-HTT–induced loss of nuclei that invariably followed the loss of neurofilament staining (**Supplementary Fig. 4b**,**c**). These experiments showed that Sirt1 directly protects neurons from mutant HTT toxicity and that Sirt1 deacetylase activity has a key role in neuroprotection.

To examine the mechanism of Sirt1-mediated neuroprotection in Huntington's disease mice, we first performed gene expression profiling in striatal samples obtained from Huntington's disease mice and Huntington's disease mice crossed with Sirt1-overexpressing mice. A Gene Set Enrichment Analysis[11] revealed that overexpression of Sirt1 in Huntington's disease mice rescued specific pathways involved in neurite development and branching (**Supplementary Fig. 5**). In addition, the mRNA level of BDNF, a key regulator of these pathways[12,13], was significantly lower in Huntington's disease mice, as previously described[14], whereas BDNF mRNA levels were significantly higher in Sirt1-KI–R6/2

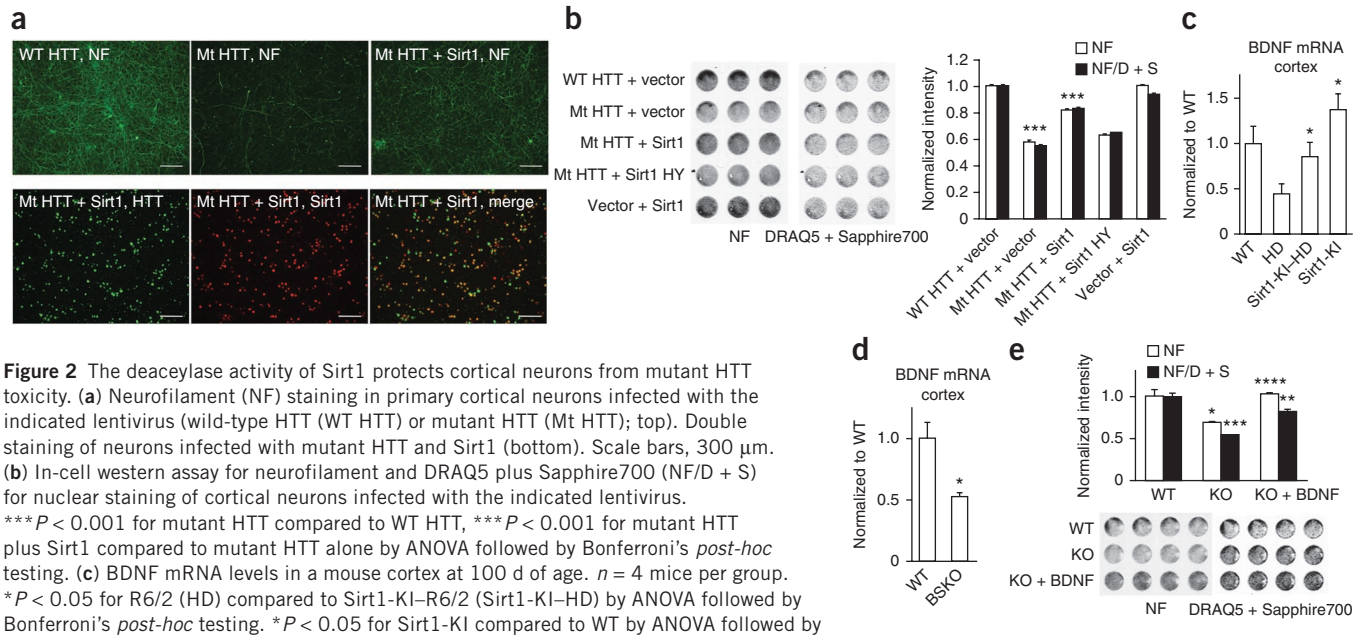

Figure 2 The deaceylase activity of Sirt1 protects cortical neurons from mutant HTT toxicity. (**a**) Neurofilament (NF) staining in primary cortical neurons infected with the indicated lentivirus (wild-type HTT (WT HTT) or mutant HTT (Mt HTT); top). Double staining of neurons infected with mutant HTT and Sirt1 (bottom). Scale bars, 300 µm. (**b**) In-cell western assay for neurofilament and DRAQ5 plus Sapphire700 (NF/D + S) for nuclear staining of cortical neurons infected with the indicated lentivirus. $^{***}P < 0.001$ for mutant HTT compared to WT HTT, $^{***}P < 0.001$ for mutant HTT plus Sirt1 compared to mutant HTT alone by ANOVA followed by Bonferroni's *post-hoc* testing. (**c**) BDNF mRNA levels in a mouse cortex at 100 d of age. $n = 4$ mice per group. $^{*}P < 0.05$ for R6/2 (HD) compared to Sirt1-KI–R6/2 (Sirt1-KI–HD) by ANOVA followed by Bonferroni's *post-hoc* testing. $^{*}P < 0.05$ for Sirt1-KI compared to WT by ANOVA followed by Bonferroni's *post-hoc* testing. (**d**) BDNF mRNA levels in a mouse cortex at 3 months of age. $n = 5$ mice per group. $^{*}P < 0.05$ by *t* test. (**e**) Toxicity in primary cortical neurons from Sirt1 knockout (KO) mice or WT littermates. $^{*}P < 0.05$ for Sirt1 knockout compared to WT Sirt1 by ANOVA followed by Bonferroni's *post-hoc* testing, $^{***}P < 0.001$ for Sirt1 knockout compared to WT by ANOVA followed by Bonferroni's *post-hoc* testing, $^{****}P < 0.001$ for Sirt1 knockout plus BDNF compared to Sirt1 knockout alone by ANOVA followed by Bonferroni's *post-hoc* testing, $^{**}P < 0.01$ for Sirt1 knockout plus BDNF compared to Sirt1 knockout alone by followed by Bonferroni's *post-hoc* testing. Error bars, ± s.e.m.

mice compared to R6/2 mice (**Fig. 2c**). In contrast, cortical brain samples from Sirt1 BSKO mice showed significantly lower levels of BDNF mRNA compared to control littermates (**Fig. 2d**), further suggesting that Sirt1 might regulate BDNF expression. Notably, experiments in primary cortical neurons isolated from the Sirt1 BKSO mice revealed that treatment with exogenous BDNF rescued the neurotoxicity observed in the Sirt1 knockout cultures (**Fig. 2e**). Taken together, these results highlight BDNF as a key target of Sirt1 function in both the normal and Huntington's disease brain and suggest that Sirt1 regulates expression of BDNF at the level of transcription.

Previous studies in primary neurons showed that CREB-mediated transcription from the BDNF promoter IV (previously known as the BDNF promoter III) accounts for most of the *BDNF* gene expression under conditions of neuronal activity[15]. Cotransfection experiments revealed significant activation of the BDNF promoter IV by Sirt1, whereas deacetylase-deficient Sirt1 did not have an effect on the activation of this promoter (**Fig. 3a**). Although CREB alone activated the promoter by about twofold, transfection of Sirt1 and CREB together resulted in synergistic 15-fold activation. Expression of a DNA-binding–incompetent form of CREB (K-CREB) did not lead to synergistic activation with Sirt1, suggesting that DNA binding by CREB is required for the synergism between Sirt1 and CREB (**Fig. 3a**). A mutant form of CREB that cannot be phosphorylated at Ser133 synergized with Sirt1, indicating that phosphorylation of CREB is not required for the synergism. A conserved family of coactivators designated 'transducers of regulated CREB activity' (TORCs) were previously identified as enhancers of CREB transcription through a phosphorylation-independent interaction with CREB[3]. We found that activation of the BDNF promoter IV by CREB was enhanced by cotransfection of CREB and TORC1 in a dose-dependent manner (**Supplementary Fig. 6a**). This effect of TORC1 was markedly potentiated by Sirt1 (**Supplementary Fig. 6a**), suggesting that Sirt1 activates the BDNF promoter IV by enhancing the CREB-TORC1 transcriptional activity.

To determine how Sirt1 potentiates CREB-TORC1 activity, we next tested whether Sirt1 interacts with each of these two factors individually. Previous studies suggested that TORC1 activated CREB-regulated transcription by promoting recruitment of the transcriptional coactivator TAF4 (ref. 3). Here we show that Sirt1 interacts with CREB, TORC1 and TAF4 (**Fig. 3b** and **Supplementary Fig. 6b**) and that expression of Sirt1 potentiated the interaction of CREB with TORC1 (**Fig. 3c**). Notably, we found that Sirt1 increased the proportion of slower-migrating TORC1 (upper band in **Fig. 3c**), which is the form of TORC1 that predominantly interacts with CREB.

Because Sirt1 is a deacetylase, we next examined whether it potentiates the TORC1-CREB interaction by deacetylating TORC1. Using an antibody to pan-acetyl lysine, we detected strong acetylation of TORC1 by CREB binding protein (CBP) but not by the catalytically inactive CBP-DY[16], where aspartic acid (D) at residue 1,435 was mutated to tyrosine (Y) (**Fig. 3d**). Notably, Sirt1, but not deacetylase-deficient Sirt1 HY, was able to deacetylate TORC1 (**Fig. 3d**). Using a mass spectrometry analysis, we identified the acetylation of several lysine residues in the TORC1 protein (**Supplementary Fig. 7**), including Lys13, Lys20, Lys33, Lys178 and Lys197. To study the functional consequences of lysine modifications, we mutated these residues, either individually or in various combinations, into arginine (LysArg), to mimic deacetylation, or glutamine (LysGln), to mimic acetylation. Although we saw no obvious effect as a result of alterations of Lys33, Lys178 or Lys197, the alterations of Lys13 and Lys20 into Arg and Gln stabilized and destabilized TORC1, respectively (**Fig. 3e**). The effects of the alterations of Lys13 and Lys20 were most notable on the slower-migrating form of TORC1 that interacts with CREB, suggesting that the acetylation or deacetylation status of Lys13 and, to a lesser degree, Lys20 has a key role in the interaction of TORC1 with CREB. Because Lys13 and Lys20 reside in the TORC1-tetramerization and CREB-binding domain[3], we hypothesized that these lysines mediate the effect of Sirt1 on the TORC1-CREB interaction and the activation of

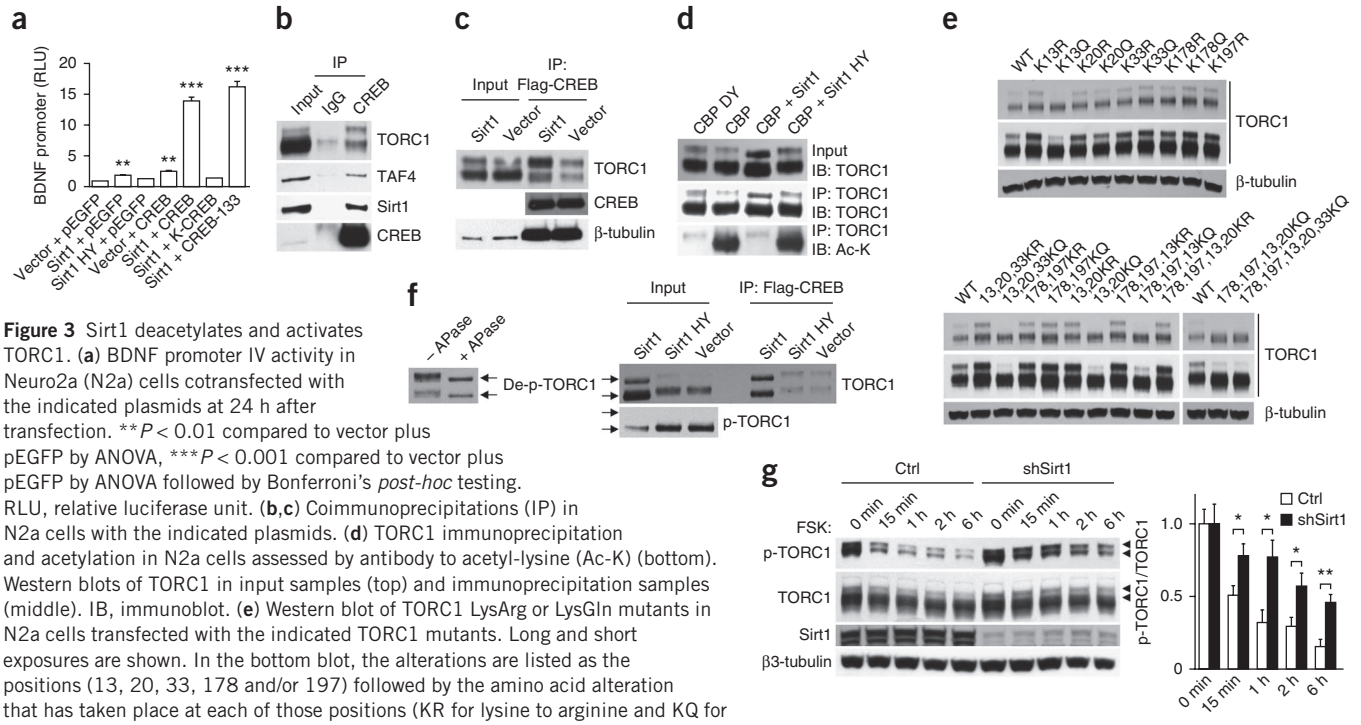

Figure 3 Sirt1 deacetylates and activates TORC1. (**a**) BDNF promoter IV activity in Neuro2a (N2a) cells cotransfected with the indicated plasmids at 24 h after transfection. $^{**}P < 0.01$ compared to vector plus pEGFP by ANOVA, $^{***}P < 0.001$ compared to vector plus pEGFP by ANOVA followed by Bonferroni's *post-hoc* testing. RLU, relative luciferase unit. (**b**,**c**) Coimmunoprecipitations (IP) in N2a cells with the indicated plasmids. (**d**) TORC1 immunoprecipitation and acetylation in N2a cells assessed by antibody to acetyl-lysine (Ac-K) (bottom). Western blots of TORC1 in input samples (top) and immunoprecipitation samples (middle). IB, immunoblot. (**e**) Western blot of TORC1 LysArg or LysGln mutants in N2a cells transfected with the indicated TORC1 mutants. Long and short exposures are shown. In the bottom blot, the alterations are listed as the positions (13, 20, 33, 178 and/or 197) followed by the amino acid alteration that has taken place at each of those positions (KR for lysine to arginine and KQ for lysine to glutamine). (**f**) Western blot of TORC1 with or without *in vitro* treatment of alkaline phosphatase (APase; left). Western blot of TORC1 and phosphorylated TORC1 (p-TORC1) and a coimmunoprecipitation assay of CREB and TORC1 in N2a cells transfected with the indicated plasmids (right). The position of TORC1 is indicated with arrows. De-p-TORC1, dephosphorylated TORC1. (**g**) Dephosphorylation of p-TORC1 by forskolin (FSK) in the presence of Sirt1 knockdown in primary cortical neurons. The position of p-TORC1 is indicated with arrowheads. $^{*}P < 0.05$, $^{**}P < 0.01$ by ANOVA followed by Bonferroni's *post-hoc* testing. ShSirt1, Sirt1 shRNA. Error bars, mean ± s.e.m.

the BDNF promoter IV. Whereas WT TORC1 or the LysArg mutants of TORC1 potentiated CREB-mediated BDNF reporter activity, the LysGln alterations at Lys13 or Lys20 showed significantly ($P < 0.01$) reduced potentiation compared to LysArg mutants (**Supplementary Fig. 8**). These results further support the notion that deacetylation of TORC1 by Sirt1 has a role in activation of BDNF transcription.

As we evaluated the TORC1 acetylation, we noted that Sirt1 gave rise to an increase in TORC1 electrophoretic mobility, an effect that was most pronounced when TORC1 was acetylated by CBP (**Fig. 3d**,**f**). Treatment of TORC1 by alkaline phosphatase revealed that the faster electrophoretic mobility forms of TORC1 generated by Sirt1 expression represented dephosphorylated TORC1 (**Fig. 3f**). Previous studies showed that cytoplasmic TORC1 is phosphorylated at Ser151 and is inactive, whereas its dephosphorylation leads to its nuclear translocation and activation[17,18]. Using primary neurons, we confirmed that the faster-migrating dephosphorylated TORC1 is the nuclear form of TORC1 (**Supplementary Fig. 9a**). Using an antibody specific to phosphorylated Ser151 (**Supplementary Fig. 9b**), we found that concentrations of phosphorylated TORC1 were greatly diminished in the presence of WT Sirt1 but not of deacetylase-deficient Sirt1, further suggesting that Sirt1 promotes the formation of dephosphorylated, active nuclear TORC1 (**Fig. 3f**).

In agreement with this conclusion, we found that knockdown of endogenous Sirt1 led to increased phosphorylation of TORC1 in primary neurons treated with forskolin[19] (**Fig. 3g**). Notably, we did not observe any changes in the concentrations of total or phosphorylated CREB in the presence of Sirt1 knockdown (**Supplementary Fig. 10**), suggesting that Sirt1 does not regulate CREB directly but, rather, through TORC1.

Together our data suggest that as part of its physiological function, Sirt1 deacetylates and activates neuronal TORC1. To determine whether mutant HTT interferes with this normal Sirt1 function, we first examined the localization of TORC1 in primary cortical neurons expressing mutant or WT HTT. Notably, expression of mutant HTT resulted in predominantly cytoplasmic localization of TORC1, suggesting that TORC1 primarily exists in its inactive, phosphorylated form in the presence of mutant HTT (**Fig. 4a**). To substantiate this conclusion *in vivo*, a chromatin immunoprecipitations (ChIP) assay revealed a significantly lower recruitment of TORC1 to the BDNF promoter IV in the cortices of R6/2 mice compared to those of WT mice (**Fig. 4b**), further suggesting that mutant HTT interferes with TORC1 nuclear localization and transcriptional activity. Moreover, we found that mutant HTT interacts with Sirt1, TORC1 (**Fig. 4c** and **Supplementary Fig. 11b**,**c**,**e**,**f**) and TAF4 (**Supplementary Fig. 11a**,**d**)[20] and it interferes with the TORC1-CREB interaction (**Supplementary Fig. 12a**,**b**). Consistent with the results shown in **Figure 4a**, we noted an increased phosphorylation of TORC1 in the presence of mutant HTT (**Supplementary Fig. 12a**), suggesting that mutant HTT, possibly through its interaction with Sirt1, interferes with the ability of Sirt1 to activate TORC1. Because TORC1 promotes the interaction of CREB with TAF4 (ref. 3), and because TAF4 has been previously implicated in CREB transcription in Huntington's disease[20], it is also possible that the interference of mutant HTT with TAF4 function contributes to transcriptional repression of the *BDNF* gene in Huntington's disease.

Because Sirt1 protected against mutant HTT toxicity and promoted the interaction of TORC1 with CREB, we examined whether expression of Sirt1 could overcome the interference of mutant HTT on the TORC1-CREB interaction. Expression of Sirt1 strongly enhanced the TORC1-CREB interaction in the presence of mutant HTT (**Supplementary Figure 12**). Based on this finding and our *in vivo*

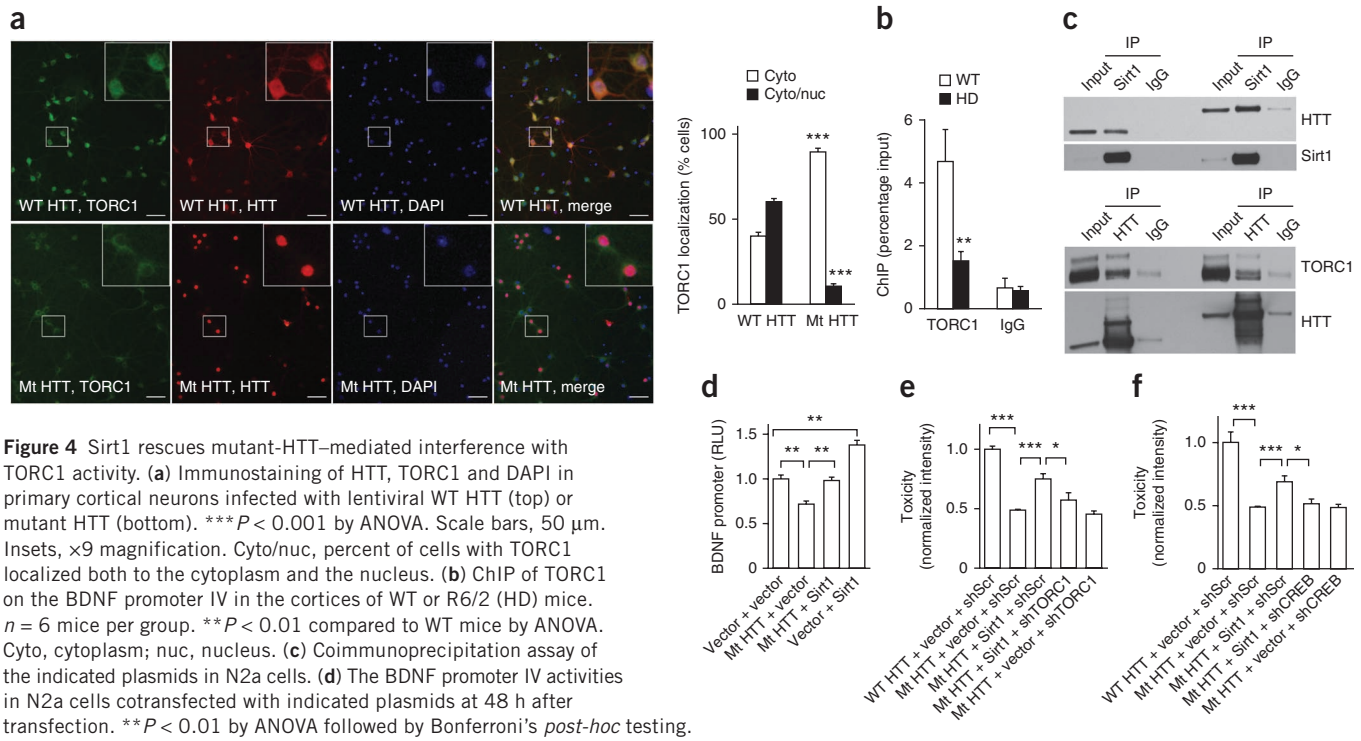

Figure 4 Sirt1 rescues mutant-HTT–mediated interference with TORC1 activity. (**a**) Immunostaining of HTT, TORC1 and DAPI in primary cortical neurons infected with lentiviral WT HTT (top) or mutant HTT (bottom). ***$P < 0.001$ by ANOVA. Scale bars, 50 µm. Insets, ×9 magnification. Cyto/nuc, percent of cells with TORC1 localized both to the cytoplasm and the nucleus. (**b**) ChIP of TORC1 on the BDNF promoter IV in the cortices of WT or R6/2 (HD) mice. $n = 6$ mice per group. **$P < 0.01$ compared to WT mice by ANOVA. Cyto, cytoplasm; nuc, nucleus. (**c**) Coimmunoprecipitation assay of the indicated plasmids in N2a cells. (**d**) The BDNF promoter IV activities in N2a cells cotransfected with indicated plasmids at 48 h after transfection. **$P < 0.01$ by ANOVA followed by Bonferroni's *post-hoc* testing. (**e**) Neurofilament staining intensity in primary cortical neurons infected with the indicated lentivirus. *$P < 0.05$ by ANOVA, ***$P < 0.001$ by ANOVA. ShScr, scramble shRNA; shTORC1, TORC1 shRNA; shCREB, CREB shRNA. (**f**) Toxicity was assessed as in **e**. *$P < 0.05$ by ANOVA followed by Bonferroni's *post-hoc* testing, ***$P < 0.001$ by ANOVA followed by Bonferroni's *post-hoc* testing. Error bars, mean ± s.e.m.

data showing the rescue of BDNF expression by Sirt1 (**Fig. 2c**), we examined whether mutant HTT and Sirt1 directly affect the transcriptional activity of the BDNF promoter IV. Previous studies showed that WT HTT upregulates the transcription of the *BDNF* gene by sequestrating the neuron-restrictive silencing factor in the cytoplasm, suggesting that the function of WT HTT has a crucial neuroprotective role in the pathogenesis of Huntington's disease[14,21]. Although those previous studies examined the BDNF promoter II, which contains the neuron-restrictive silencing factor binding site, our study examined the BDNF promoter IV, which is regulated by CREB[15]. We found that mutant HTT, but not WT HTT, interfered with the Sirt1-mediated activation of the transcription from the BDNF promoter IV (**Supplementary Fig. 12c**). Notably, expression of Sirt1 resulted in a significant reversal of mutant-HTT–mediated repression of the BDNF promoter IV (**Fig. 4d**), further suggesting that Sirt1 can rescue the effect of mutant HTT on BDNF transcription.

In light of our results suggesting that TORC1 has a crucial role in Sirt1-mediated protection from mutant HTT toxicity, we directly examined whether Sirt1 protection depends on the presence of TORC1. To this end, we transduced primary cortical neurons with lentivirally expressed mutant HTT and Sirt1 in the presence or absence of TORC1 knockdown. Using a lentiviral shRNA approach, about 70% knockdown of TORC1 was achieved that was not itself neurotoxic (**Supplementary Fig. 13a**,**b**). Notably, Sirt1 rescue of mutant HTT toxicity was significantly compromised in the presence of TORC1 knockdown (**Fig. 4e**), suggesting that expression of TORC1 is at least in part required for Sirt1-mediated neuroprotection. Finally, we hypothesized that if Sirt1 primarily protects from mutant HTT toxicity by activating TORC1 and, consequently, CREB, the knockdown of CREB would also be expected to diminish Sirt1 rescue. Using a CREB shRNA (shCREB) lentivirus to achieve nontoxic knockdown of CREB at baseline, we found that the Sirt1-mediated rescue of mutant HTT toxicity was completely dependent on the presence of endogenous CREB (**Fig. 4f** and **Supplementary Fig. 13c**). These results strengthen the conclusion that the TORC1-CREB pathway has a crucial role in mediating Sirt1 neuroprotection in neurons expressing mutant HTT.

We show here that Sirt1 has a key neuroprotective role in the pathogenesis of Huntington's disease. Using primary neurons, we confirmed that Sirt1 directly targets neurons to mediate neuroprotection against mutant HTT. Our data show that under normal conditions, Sirt1 promotes the deacetylation of TORC1 and its interaction with CREB, which leads to activation of target genes such as *BDNF*. Mutant HTT interacts with Sirt1 and interferes with the Sirt1-mediated activation of TORC1, which, in turn, results in transcriptional repression. Notably, overexpression of Sirt1 rescued this effect of mutant HTT *in vitro* and *in vivo*.

Our finding that Sirt1 confers neuroprotection in R6/2 mice is in agreement with the accompanying manuscript[22], in which Sirt1-mediated neuroprotection was observed in another fragment model (termed 171aa) and in a full-length Huntington's disease mouse model. Notably, Sirt1 overexpression did not affect survival time or the aggregation of mutant HTT in 171aa mice despite the observed neuroprotection it conferred. Although the reasons for these discrepancies are unknown, it is notable that 171aa mice developed hyperinsulinemia and insulin resistance, which we did not see in the R6/2 model that we used. Several published reports implicate insulin signaling in the regulation of the aggregation of mutant HTT and proteotoxicity, but its role in neurodegeneration is unresolved[23]. It is therefore possible that hyperinsulinemia in 171aa mice contributes to the differences in survival time and the aggregation of mutant HTT after Sirt1 rescue. Although it is not precisely known why Huntington's disease model mice die, recent work[24] showed that *HTT* fragment models (R6/2 and 171aa) develop profound hypothermia that presumably contributes to

death in these mice. As hypothermia does not seem to have a similar role in humans with Huntington's disease, it can therefore be argued that survival as an outcome measure in Huntington's disease model mice may not directly inform about human disease. However, it is generally accepted that the striatal and neuronal atrophy observed in Huntington's disease model mice strongly resembles that seen in human disease, and on this key measure, our study is in agreement with the accompanying study[22].

We identified TORC1 as a previously unknown target of Sirt1 deacetylase, whereas the accompanying study[22] showed that previously known substrates of Sirt1, such as FoxO3a and p53, were also altered in Huntington's disease models. Because mutant HTT partially inhibits Sirt1 deacetylase activity[22], it is not surprising that multiple substrates of Sirt1 showed increased acetylation in Huntington's disease models. Notably, overexpression of Sirt1 was able to overcome this inhibition and partially correct the acetylation status of the Sirt1 substrates. In light of our data indicating that TORC1 is required for Sirt1-mediated rescue of mutant HTT toxicity, it will be of interest to further examine possible links between TORC1 and other Sirt1 substrates in Huntington's disease. As a regulator of neuronal-activity–dependent CREB transcription, TORC1 presumably regulates other Cre-regulated genes that have previously been implicated in the pathogenesis of Huntington's disease. For example, recent studies have suggested that TORC1 activates the transcription of PGC-1α[25], which is a master regulator of mitochondrial function that has been implicated in the pathogenesis of Huntington's disease[24,26] and other neurodegenerative disorders[27–30]. In support of this notion, we found that Sirt1 significantly ($P < 0.01$) rescued expression of PGC-1α in R6/2 mice (**Supplementary Fig. 14**). The regulatory regions of the *FoxO3* gene contain a Cre site[31], suggesting that TORC1 may also regulate FoxO3a expression. It will therefore be of interest to examine whether Sirt1 deacetylation of TORC1 leads to the activation of multiple target genes in the central nervous system. Because TORC1 is essentially brain specific[18], it can be used to monitor the function of Sirt1 in neurons, especially in the context of therapeutic interventions. Together, our results suggest that pharmacological targeting of Sirt1 could provide an opportunity for therapeutic development in Huntington's disease.

METHODS

Methods and any associated references are available in the online version of the paper at http://www.nature.com/naturemedicine/.

Note: Supplementary information is available on the Nature Medicine website.

ACKNOWLEDGMENTS

We thank M. Montminy (Peptide Biology Laboratories (PBL), Salk Institute) for the Flag-CREB, Flag-TORC1 and Flag-TORC1 S151A plasmids and for antibody to TORC1 (#6937, PBL, Salk Institute) and helpful discussions; M.E. Greenberg (Harvard Medical School) for the pIII(170)Luc plasmid[15]; T. Kouzarides (University of Cambridge) for Sirt1 and Sirt1 HY plasmids; Z. Wu (Novartis Institutes for Biomedical Research) for the TORC1 plasmid; M. Difiglia (Massachusetts General Hospital) for antibody to HTT (Ab1); E. Regulier (Novartis Institutes for Biomedical Research) for lentiviral vectors expressing *HTT*Ex1-25Q, *HTT*Ex1-72Q and Sirt1; and J.M. Park (Massachusetts General Hospital) for the lentiviral vector used for CREB knockdown. We also acknowledge C. Whitaker (Massachusetts Institute of Technology) for analysis of the microarray data. This work was supported by grant R01NS051303 from the US National Institutes of Health (D.K.); the Cure Huntington's Disease Initiative (CHDI), Hereditary Disease Foundation (HDF) (D.E.C.); US National Institutes of Health, Glenn Foundation for Medical Research (L.G.) and grants R01MH067880-08 and P41RR011823-15 from the US National Institutes of Health (J.R.Y.).

AUTHOR CONTRIBUTIONS

H.J. performed the experiments shown in **Figures 2–4** and **Supplementary Figures 4**, **6** and **9–13**. D.E.C. and A.S. performed the experiments shown in **Figures 1a**, **1e**, **2c** and **2d** and **Supplementary Figures 1** and **5**. L.C. performed the experiments shown in **Figure 1b–h** and **Supplementary Figures 13** and **14**. J.R.M. helped with the experiments shown in **Figure 4f**. J.N.S. and J.R.Y. performed the experiments shown in **Supplementary Figure 7**. L.B. performed the experiments shown in **Supplementary Figure 2**. L.P.G. and D.K. provided the conceptual framework for the study and discussed the results. D.K. and H.J. wrote the paper.

COMPETING FINANCIAL INTERESTS

The authors declare competing financial interests: details accompany the full-text HTML version of the paper at http://www.nature.com/naturemedicine/.

Published online at http://www.nature.com/naturemedicine/.
Reprints and permissions information is available online at http://www.nature.com/reprints/index.html.

1. Haigis, M.C. & Guarente, L.P. Mammalian sirtuins–emerging roles in physiology, aging, and calorie restriction. *Genes Dev.* **20**, 2913–2921 (2006).
2. Gatchel, J.R. & Zoghbi, H.Y. Diseases of unstable repeat expansion: mechanisms and common principles. *Nat. Rev. Genet.* **6**, 743–755 (2005).
3. Conkright, M.D. *et al.* TORCs: transducers of regulated CREB activity. *Mol. Cell* **12**, 413–423 (2003).
4. Pallos, J. *et al.* Inhibition of specific HDACs and sirtuins suppresses pathogenesis in a *Drosophila* model of Huntington's disease. *Hum. Mol. Genet.* **17**, 3767–3775 (2008).
5. Parker, J.A. *et al.* Resveratrol rescues mutant polyglutamine cytotoxicity in nematode and mammalian neurons. *Nat. Genet.* **37**, 349–350 (2005).
6. Cohen, D.E., Supinski, A.M., Bonkowski, M.S., Donmez, G. & Guarente, L.P. Neuronal SIRT1 regulates endocrine and behavioral responses to calorie restriction. *Genes Dev.* **23**, 2812–2817 (2009).
7. Mangiarini, L. *et al.* Exon 1 of the HD gene with an expanded CAG repeat is sufficient to cause a progressive neurological phenotype in transgenic mice. *Cell* **87**, 493–506 (1996).
8. Stack, E.C. *et al.* Chronology of behavioral symptoms and neuropathological sequela in R6/2 Huntington's disease transgenic mice. *J. Comp. Neurol.* **490**, 354–370 (2005).
9. Bordone, L. *et al.* SIRT1 transgenic mice show phenotypes resembling calorie restriction. *Aging Cell* **6**, 759–767 (2007).
10. Zala, D. *et al.* Progressive and selective striatal degeneration in primary neuronal cultures using lentiviral vector coding for a mutant huntingtin fragment. *Neurobiol. Dis.* **20**, 785–798 (2005).
11. Subramanian, A. *et al.* Gene set enrichment analysis: a knowledge-based approach for interpreting genome-wide expression profiles. *Proc. Natl. Acad. Sci. USA* **102**, 15545–15550 (2005).
12. Greenberg, M.E., Xu, B., Lu, B. & Hempstead, B.L. New insights in the biology of BDNF synthesis and release: implications in CNS function. *J. Neurosci.* **29**, 12764–12767 (2009).
13. Chao, M.V., Rajagopal, R. & Lee, F.S. Neurotrophin signalling in health and disease. *Clin. Sci. (Lond.)* **110**, 167–173 (2006).
14. Zuccato, C. *et al.* Loss of huntingtin-mediated *BDNF* gene transcription in Huntington's disease. *Science* **293**, 493–498 (2001).
15. Tao, X., Finkbeiner, S., Arnold, D.B., Shaywitz, A.J. & Greenberg, M.E. $Ca2^{+}$ influx regulates BDNF transcription by a CREB family transcription factor-dependent mechanism. *Neuron* **20**, 709–726 (1998).
16. Jeong, H. *et al.* Acetylation targets mutant huntingtin to autophagosomes for degradation. *Cell* **137**, 60–72 (2009).
17. Bittinger, M.A. *et al.* Activation of cAMP response element–mediated gene expression by regulated nuclear transport of TORC proteins. *Curr. Biol.* **14**, 2156–2161 (2004).
18. Altarejos, J.Y. *et al.* The Creb1 coactivator Crtc1 is required for energy balance and fertility. *Nat. Med.* **14**, 1112–1117 (2008).
19. Li, S., Zhang, C., Takemori, H., Zhou, Y. & Xiong, Z.Q. TORC1 regulates activity-dependent CREB-target gene transcription and dendritic growth of developing cortical neurons. *J. Neurosci.* **29**, 2334–2343 (2009).
20. Dunah, A.W. *et al.* Sp1 and TAFII130 transcriptional activity disrupted in early Huntington's disease. *Science* **296**, 2238–2243 (2002).
21. Zuccato, C. *et al.* Huntingtin interacts with REST/NRSF to modulate the transcription of NRSE-controlled neuronal genes. *Nat. Genet.* **35**, 76–83 (2003).
22. Jiang, M. *et al.* Neuroprotective role of SIRT1 in mammalian models of Huntington's disease through activation of multiple SIRT1 targets. *Nat. Med.* advance online publication, doi:10.1038/nm.2558 (18 December 2011).
23. Cohen, E. & Dillin, A. The insulin paradox: aging, proteotoxicity and neurodegeneration. *Nat. Rev. Neurosci.* **9**, 759–767 (2008).
24. Weydt, P. *et al.* Thermoregulatory and metabolic defects in Huntington's disease transgenic mice implicate PGC-1α in Huntington's disease neurodegeneration. *Cell Metab.* **4**, 349–362 (2006).
25. Wu, Z. *et al.* Transducer of regulated CREB-binding proteins (TORCs) induce PGC-1α transcription and mitochondrial biogenesis in muscle cells. *Proc. Natl. Acad. Sci. USA* **103**, 14379–14384 (2006).

26. Cui, L. *et al.* Transcriptional repression of PGC-1α by mutant huntingtin leads to mitochondrial dysfunction and neurodegeneration. *Cell* **127**, 59–69 (2006).
27. Beal, M.F. Mitochondria and neurodegeneration. *Novartis Found. Symp.* **287**, 183–192 (2007).
28. Wang, J. *et al.* The role of Sirt1: at the crossroad between promotion of longevity and protection against Alzheimer's disease neuropathology. *Biochim. Biophys. Acta* **1804**, 1690–1694 (2010).
29. Zhao, W. *et al.* Peroxisome proliferator activator receptor γ coactivator-1α (PGC-1α) improves motor performance and survival in a mouse model of amyotrophic lateral sclerosis. *Mol. Neurodegener.* **6**, 51 (2011).
30. Zheng, B. *et al.* PGC-1α, a potential therapeutic target for early intervention in Parkinson's disease. *Sci. Transl. Med.* **2**, 52ra73 (2010).
31. Zhang, X. *et al.* Genome-wide analysis of cAMP-response element binding protein occupancy, phosphorylation, and target gene activation in human tissues. *Proc. Natl. Acad. Sci. USA* **102**, 4459–4464 (2005).

ONLINE METHODS

Mouse studies. To generate BSKO-R6/2 mice, *Sirt1*$^{flox/flox}$; Nestin-Cre mice and R6/2 mice were intercrossed for two generations. Nestin-Cre was always passed through the male germline. The crosses were all carried out on a C57BL/6 background. R6/2 mice on the C57BL6/J background were obtained from PsychoGenics. Sirt1-KI–R6/2 mice were generated by intercrossing mice heterozygous for the Sirt1-KI transgene, maintained on an outbred background[9], with R6/2 mice on the B6CBAF1/J background (Jackson Laboratories). Rotarod analysis was performed using a Rotamex-5 Rota Rod apparatus (Columbus Instruments). For the neuropathological analyses, we examined brain sections stereologically, as described[26]. We used the dissector-counting method to assess striatal neurons and mutant-HTT–positive aggregates using an unbiased random selection of serial sections in a defined volume of the neostriatum, as described[8]. These studies were approved by the Massachusetts General Hospital Subcommittee on Research Animal Care and the Committee on Animal Care at the Massachusetts Institute of Technology.

Quantitative RT-PCR. Quantitative RT-PCR was performed using iQ SYBR Green Supermix (Bio-Rad Laboratories) on a Light Cycler 480 II (Roche). The primers used were: BDNF forward: 5′- TCATACTTCGGTTGCATGAAGG-3′; BDNF reverse: 5′-AGACCTCTCGAACCTGCCC-3′; and 18S forward and 18S reverse obtained from the Harvard Primer Bank[32]. Relative mRNA abundance was calculated using the ΔΔCT method.

Plasmids and antibodies. Lentiviral transfer vectors *HTT*Ex1-25Q, *HTT*Ex1-72Q, BDNF-luciferase construct (pIII(170)Luc)[15], Sirt1 and Sirt1 HY plasmids, Flag-CREB, TORC1, Flag-TORC1 and Flag-TORC1 S151A[3] were described previously. CREB, K-CREB, CREB-133 and pEGFP were purchased from Clontech. Human *HTT*Ex1 25Q-GFP, *HTT*Ex1-103Q-GFP, *HTT*480-17stop, *HTT*480-68stop, HA-TAF and CBP-HAT constructs were described previously[16]. ShRNA lentiviral plasmids (pLKO.1) targeting Sirt1 (5′-AAGTTGACCTCCTCATTGTTA-3′) and TORC1 (5′-TTGATTCAGACCATCAGTTTC-3′) were purchased from Sigma. Lentiviral Sirt1 HY was generated by altering His363 to Tyr363. We used primary antibodies to the following: neurofilament (2H3, Developmental Studies Hybridoma Bank), Flag (F7425, Sigma), Flag M2 (F3165, Sigma), HA (HA.11, Covance, 3724, Cell Signaling), TORC1 (2587, Cell Signaling Technology, 6937 from M. Montminy, Peptide Biology Laboratories, the Salk Institute), phosphorylated S151 TORC1 (3359, Cell Signaling Technology), Myc (2276, Cell Signaling Technology, sc-789, Santa Cruz, MCA1929, serotec), acetyl lysine (ICP0380, Immunechem), Sirt1 (07-131, Upstate, sc-15404, Santa Cruz, 2028, Cell Signaling and custom-made Sirt1 antibody from L.G.), β-tubulin (T4026, Sigma), β3-tubulin (4466, Cell Signaling Technology) and HTT (MAB5492 and MAB2166, Millipore and Ab1 from M. Difiglia, Department of Neurology, Massachusetts General Hospital).

Primary neurons. Rat and mouse embryonic primary cortical neurons prepared from embryonic day (E) 19 and E17 embryos, respectively, were infected with lentiviral vectors at a multiplicity of infection of 3 on *in vitro* day (DIV) 4. Lentivirus was produced as previously described[33]. Neurons fixed and double stained with antibody to neurofilament and with DRAQ5 plus Sapphire700 were analyzed using the Odyssey Infrared Imaging System (LI-COR Biosciences). Sirt1 knockout and WT cultures were prepared by dissecting and plating each embryo from E16 littermates separately. BDNF was added to Sirt1 knockout culture at 50 ng ml^{-1} every other day starting at DIV5. For knockdown of Sirt1, neurons were infected with shRNA scrambled or shRNA Sirt1 lentivirus at multiplicity of infection of 1 on DIV8. At 5 d after infection (DIV13), neurons were treated with 25 μM forskolin.

Reporter assays and coimmunoprecipitations. N2a cells cultured in DMEM with 10% FBS were transfected using Lipofectamine 2000. Transfected cells were harvested at 24 h after transfection, unless otherwise specified. For coimmunoprecipitation, transfected N2a cells were harvested at 24 h after transfection, and coimmunoprecipitation was performed as previously described[34]. For the luciferase reporter assays, we used 50 ng of reporter in each well of 24-well plates. We prepared cell extracts 24–48 h after transfection, and performed the luciferase assay following standard protocol. For the alkaline phosphatase treatment, we immunoprecipitated N2a cells cotransfected with Flag-CREB and TORC1 with antibodies to Flag. We carried out dephosphorylation reactions on coimmunoprecipitated TORC1-containing protein G beads.

Multidimensional Protein Identification Technology (MudPIT) and LTQ Orbitrap mass spectromtery. RAW files were extracted with RAW_Extract and uploaded to Integrated Proteomics Pipeline-IP2 software. Tandem mass spectrometry spectra were searched with Prolucid algorithm (EBI-IPI_Human_3_30_06-28-2007) concatenated to a reverse decoy database[35]. Searches were performed with Cysteine carbamidomethylation as a fixed modification, and Lysine acetylation was searched as a differential modification (42.01056 Da). We assembled and filtered the ProLuCID[36] results using the DTA Select (version 2.0) program[37]. We assessed the validity of the peptide-spectrum matches using the SEQUEST-defined parameters, with linear discriminate analysis to dynamically set XCorr and DeltaCN thresholds for the dataset to achieve a 5% protein false discovery rate[38].

ChIP assays. We performed ChIP assays of mouse brains using the Magna ChIP kit (Millipore) according to manufacturer's protocol using antibody to TORC1 (6937, PBL, the Salk Institute) and normal rabbit IgG (Santa Cruz). The primer sequences for the BDNF promoter IV were published previously[39].

Site-directed mutagenesis of TORC1. We generated TORC1 mutants using a QuikChange II XL Site-Directed Mutagenesis Kit (Agilent). We verified incorporation of the mutations by DNA sequencing (Massachusetts General Hospital DNA Sequencing Core).

Additional methods. Detailed methodology is described in the **Supplementary Methods**.

32. Spandidos, A., Wang, X., Wang, H. & Seed, B. PrimerBank: a resource of human and mouse PCR primer pairs for gene expression detection and quantification. *Nucleic Acids Res.* **38**, D792–D799 (2010).
33. Tiscornia, G., Singer, O. & Verma, I.M. Production and purification of lentiviral vectors. *Nat. Protoc.* **1**, 241–245 (2006).
34. Sarbassov, D.D. *et al.* Rictor, a novel binding partner of mTOR, defines a rapamycin-insensitive and raptor-independent pathway that regulates the cytoskeleton. *Curr. Biol.* **14**, 1296–1302 (2004).
35. Peng, J., Elias, J.E., Thoreen, C.C., Licklider, L.J. & Gygi, S.P. Evaluation of multidimensional chromatography coupled with tandem mass spectrometry (LC/LC-MS/MS) for large-scale protein analysis: the yeast proteome. *J. Proteome Res.* **2**, 43–50 (2003).
36. Yates, J.R. III, Eng, J.K., McCormack, A.L. & Schieltz, D. Method to correlate tandem mass spectra of modified peptides to amino acid sequences in the protein database. *Anal. Chem.* **67**, 1426–1436 (1995).
37. Tabb, D.L., McDonald, W.H. & Yates, J.R. III. DTASelect and Contrast: tools for assembling and comparing protein identifications from shotgun proteomics. *J. Proteome Res.* **1**, 21–26 (2002).
38. MacCoss, M.J., Wu, C.C. & Yates, J.R. III. Probability-based validation of protein identifications using a modified SEQUEST algorithm. *Anal. Chem.* **74**, 5593–5599 (2002).
39. Gao, J. *et al.* A novel pathway regulates memory and plasticity via SIRT1 and miR-134. *Nature* **466**, 1105–1109 (2010).

doi:10.1038/nm.2559